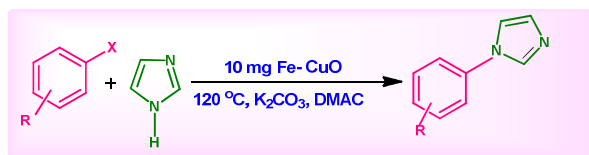




Magnetically Retrievable Lepidocrocite Supported Copper Oxide Nanocatalyst (Fe–CuO) for N–Arylation of Imidazole

Journal:	<i>RSC Advances</i>
Manuscript ID:	RA-ART-10-2014-013256.R1
Article Type:	Paper
Date Submitted by the Author:	07-Dec-2014
Complete List of Authors:	Rajaram, Sivakami; Bharathidasan university, School of Physics Babu, S; SRM Research Institute, SRM University, Chemistry Sivasubramanian, Dhanuskodi; Bharathidasan University, School of Physics Karvembu, R; National Institute of Technology, Chemistry

Graphical abstract



A novel magnetically separable γ -FeOOH supported CuO is prepared by a simple precipitation method and is found to be an effective and reusable heterogeneous catalyst for ligand-free N-arylation reaction.

Research Highlights

- Fe-CuO catalyst is prepared by simple precipitation method and this catalyst is cheap, highly efficient, stable, magnetically retrievable and reusable.

Magnetically Retrievable Lepidocrocite Supported Copper Oxide Nanocatalyst (Fe–CuO) for N–Arylation of Imidazole

R. Sivakami^a, S. Ganesh Babu^c, S. Dhanuskodi^{*a}, R. Karvembu^{*b}

Received (in XXX, XXX) Xth XXXXXXXXX 20XX, Accepted Xth XXXXXXXXX 20XX

5 DOI: 10.1039/b000000x

A simple and efficient lepidocrocite-supported copper oxide catalyst (Fe-CuO) has been successfully prepared by a simple precipitation method in aqueous medium from readily available inexpensive starting materials and was used as a heterogeneous nanocatalyst for the N-arylation of imidazole with various aryl halides. The morphology, crystal structure, magnetic property, chemical state and surface area of the catalyst were studied. The N-arylation reaction was chosen to demonstrate the catalytic efficiency of the prepared Fe-CuO. Importantly, the catalyst can be easily recovered by magnetic attraction and its catalytic activity remains unaltered even after 6 consecutive cycles. Hence, Fe-CuO is environmental friendly, easily applicable and cost effective catalyst.

Introduction

Transition-metals-catalyzed cross-coupling reactions represent one of the robust methods for the formation of carbon-carbon and carbon-heteroatom bonds¹. Particularly, the synthesis of N-arylimidazole attracted significant interest because of the frequent occurrence of these structural units in biologically active inhibitors². N-Arylimidazole is not only important in biological systems but also a common moiety in pharmaceutical research. A significant number of N-arylimidazole derivatives has been reported to have biomedical applications; serve as cyclic AMP phosphodiesterase inhibitors³, AMPA receptor antagonists⁴, cardio tonic agents⁵, thromboxane synthases inhibitors⁶ and topical antiglaucoma agents⁷. Therefore, their preparation has been attracted much attention. In recent years, the homogeneous Pd-catalyzed N-arylation of imidazole has made remarkable achievements, and performed under relatively mild reaction conditions⁸. In spite of having wide scope and excellent compatibility with many functional groups, these protocols often suffer from the disadvantages resulting from (i) the high cost of the Pd precursors, (ii) the need for ancillary ligands, (iii) the toxicity of Pd salts and (iv) the extended reaction times.

^a School of Physics, Bharathidasan University, Tiruchirappalli-620 024, India, E-mail: dhanus2k3@yahoo.com

^b Department of Chemistry, National Institute of Technology, Tiruchirappalli - 620 015, India, E-mail: kar@nitt.edu

For Electronic supplementary information (ESI) available see DOI:

In addition, higher stoichiometric amounts of Pd catalyst are often required. To circumvent these issues, newer and milder homogeneous transition metal catalysts have been developed. The major drawback of homogeneous catalysts is difficulty in separation from the product and/or reaction medium and thus product purification, recovery and regeneration of catalyst are very difficult⁹. Nowadays, heterogeneous catalysts particularly metal nanoparticles (MNPs) including CuO with high surface area are getting so much attention from both economic and industrial point of view because they possess very good activity and are highly recyclable¹⁰⁻¹¹. Despite of their advantages, drawbacks remain in these catalysts too, as the metal nanoparticles effortlessly agglomerate during the reaction and are less stable under severe reaction conditions, which lead to low catalytic activity as well as poor reusability of the catalysts¹². To prevent the agglomeration of metal nanoparticles and the over-stoichiometric use of Cu reagents, several inorganic materials such as alumina and silica have been used as a support for metal nano particles, but again they have limited stability under both acidic and basic conditions¹³. Therefore, developing an efficient and recyclable catalyst for the N-arylation of heterocycles with the use of lower amount of Cu remains a challenging one. Magnetically active nano particles have recently emerged as viable alternatives to conventional catalyst supports¹⁴⁻¹⁵. On the other hand, magnetic nanocomposites serve both as the support and stabilizer for the nanoparticles, thus providing a better chance

to prevent aggregation. Furthermore, magnetic separation is an alternative to filtration or centrifugation as it prevents loss of catalyst and increases the reusability¹⁶. Iron oxides, such as magnetite, hematite and some other iron oxides have been well investigated as catalysts or supports in various important organic transformations¹⁷⁻²⁰. For instance, copper on iron oxide was used for the synthesis propargylamines²¹ and Pd-magnetite was exploited in carbonylative Sonogashira coupling reaction²². In recent years, copper based catalysts/nanocatalysts are widely employed in various organic processes and catalytic reactions²³⁻²⁶ including energy conversion²⁷. However less attention has been focused on the catalytic applications of Fe–CuO. We believe that Fe–CuO magnetic nanocatalyst could overcome the drawbacks exist in the N-arylation of heterocycles. Herein we describe an inexpensive, stable, magnetically separable and recyclable Fe–CuO nanocatalyst for N-arylation reaction of imidazole with various aryl halides under ligand-free condition. This system provided a simplified procedure for the isolation of the catalyst.

Results and discussion

The lepidocrocite and Fe–CuO were prepared following a literature method²⁸. After drying the resulting material, the initial investigation was focused on the characterization of the resulting new solid material. Based on the inductively coupled plasma optical emission spectrometer (ICP-OES) analysis, the amount of Cu and Fe were 0.431 and 0.602 mol/g respectively in Fe-CuO.

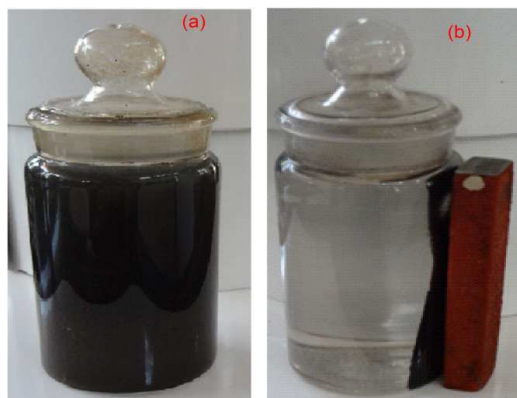


Fig. 1 Photograph of the (a) catalyst dispersed in the reaction mixture and (b) magnetic separation of the catalyst from the reaction medium.

The crystallinity of the γ -FeOOH and Fe-CuO was examined by powder X-ray diffraction. The XRD peaks correspond to single orthorhombic phase. The crystallite size of

the γ -FeOOH and Fe-CuO was found to be 47 and 41 nm (calculated using Scherrer's equation).

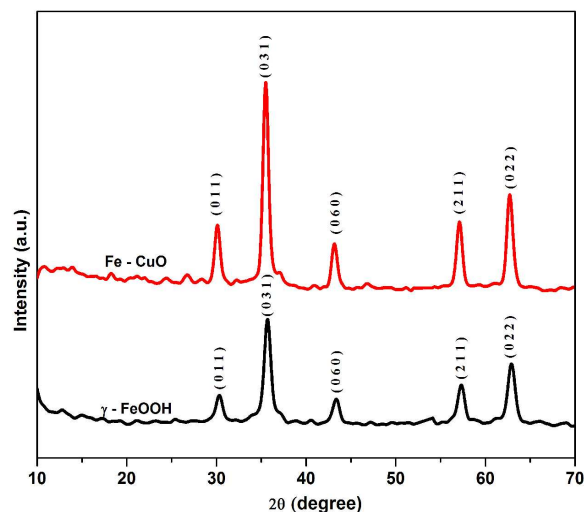


Fig. 2 XRD patterns of γ -FeOOH and Fe-CuO.

FT-IR confirms the Cu substitution in the γ -FeOOH nanoparticles (see ESI- S1†). SEM images of γ -FeOOH and γ -FeOOH supported CuO reveal the compact arrangement of nanoparticles with spherical shape (see ESI – S2†). Elemental composition obtained from the EDAX analysis shows that the weight percentage of Cu is around 4.9 in Fe-CuO. TEM images revealed that the particle size of as prepared and calcined at 500°C for 3h Fe-CuO nanocomposites (Fig. 5). Images showed agglomeration of the nanoparticles, which may be attributed to the interactions among the magnetic particles³³. The Fe - CuO powder showed particle sizes ranging from 7 and 32 nm.

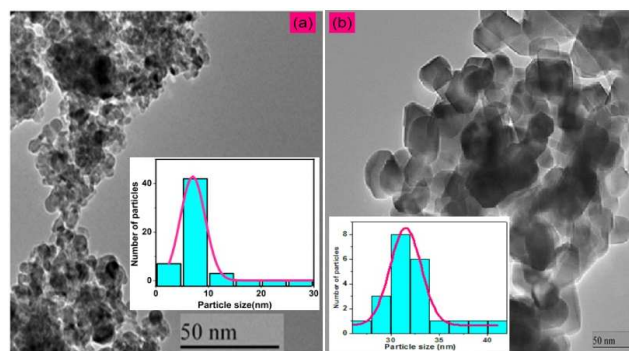


Fig. 5 TEM images of Fe-CuO nanocatalyst (a) as prepared and (b) calcined at 500°C for 3h [inset is the particle size distribution]

XPS spectra of Fe-CuO are displayed in Fig. (6(i-iv)). As seen in (Fig. 6(i)), the wide XPS spectrum reveals the presence of Fe,

Cu and O elements. The curve fitting was performed on Fe, Cu and O1s spectra of Fe-CuO using a Gaussian–Lorentzian peak shape. (Fig. 6(ii)) shows the Fe 2p core level spectra. The peaks located at 713.39 eV for Fe 2p_{3/2} and 726.02 eV for Fe 2p_{1/2} were ascribed to the presence of Fe³⁺ ions in FeOOH. These values are in good agreement with the reported data³⁴.

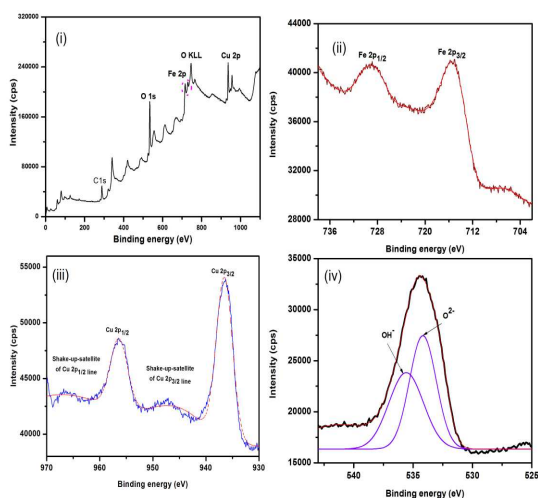


Fig. 6 XPS spectra of Fe-CuO nanocatalyst (i) XPS survey spectrum, (ii) main peaks of Fe 2p (iii) main peaks of Cu 2p and (iv) O 1s spectra

In (Fig. 6(iii)), the peaks at the binding energies of 956.2 and 936.3 eV accompanying with their shakeup satellites, correspond to Cu2p_{1/2} and Cu 2p_{3/2}, which proved the presence of Cu²⁺ ions³⁵ and thereby confirmed the formation of CuO. In fact, the shake-up satellite feature is peculiar to CuO that relates to d⁹ configuration of ground state of the Cu. Fitting of the oxygen region produced two O 1s peaks. In (Fig. 6(iv)), the peak at 530.80 eV corresponds to O²⁻ in the lattice. Similarly the peak at 532.54 eV is due to surface hydroxyl groups or chemisorbed water molecules³⁶. The peak at 289eV is attributed to C1s spectra. This proves there has been a strong interaction between lepidocrocite and CuO nanoparticles.

The Raman spectrum (see ESI – S3†) confirms the presence of Fe and Cu nanoparticles in the structure of the material. The band positions of the Fe and Cu phases are in excellent match with the literature values³⁷⁻³⁸. Thermal stability of the catalyst was found with TG /DTA analysis and found to be stable up to 1000°C³⁹⁻⁴¹ (see ESI – S3†).

The ferromagnetic behaviour was confirmed using magnetization curves of γ- FeOOH and Fe-CuO at room temperature. The observed saturation magnetization (Ms) and coercivity (Hc) values have been summarized in Table [inset Fig. 8] (see ESI – S5†). The increase of saturation magnetization for CuO loaded sample is due to the higher surface electron spins. The CuO added sample showed reduction in coercive field. This may be due to the effect of CuO into the domains of γ-FeOOH⁴².

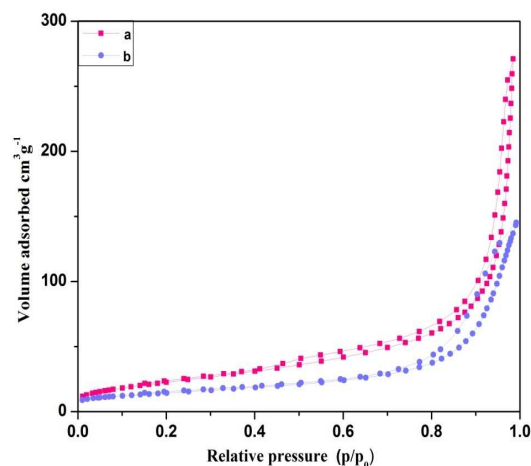
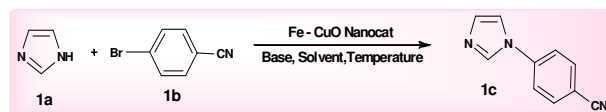


Fig. 10 N2 adsorption–desorption isotherm of (a) prepared and (b) Calcined Fe-CuO Nanocatalyst

Table 2 Optimization of the reaction conditions for the Fe-CuO–catalyzed N-arylation of imidazole (1a) with 4- bromobenzonitrile (1b) to obtain N-arylated imidazole (1c)^a



Entry	Solvent	Base	Time (h)	Temperature (°C)	Yield ^b (%)
1	DMF	K ₂ CO ₃	10	70	16
2	DMSO	K ₂ CO ₃	8	80	18
3	DMAc	K ₂ CO ₃	30	140	53
4	CH ₃ CN	KOH	12	110	3
5	DMAc	-	24	110	NR
6	DMAc	CS ₂ CO ₃	20	40	7
7	DMAc-H ₂ O	NaOH	6	50	3
8	DMAc	K ^t -OBu	10	80	9
9	DMAc	K ₃ PO ₄	15	75	5
10	DMAc	K ₃ PO ₄	22	60	6
11	DMAc	K ₂ CO ₃	24	120	83
12	DMAc	K ₂ CO ₃	16	100	71
13	DMAc	K ₂ CO ₃	40	110	77

^a All the reactions were performed with Fe-CuO (10 mg), 1 mmol (182 mg) of 4-bromobenzonitrile, 1.2 mmol (81 mg) of imidazole, and 2.0 mmol of base in 4 mL of solvent at 120 °C for 24 h. ^b GC yield, NR = No reaction

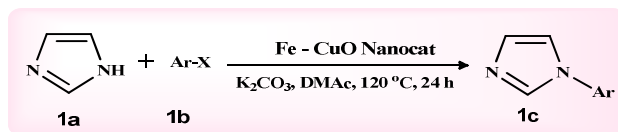
After the successful preparation and characterization of Fe-CuO, its catalytic activity was examined for N-arylation of imidazole with 4-bromobenzonitrile. Initially, the reaction conditions such as base, solvent, reaction time and reaction temperature are optimized. The results showed that 120 °C was required for the coupling reaction to give 83% yield (Table 2, entry 12) of the product. Shorter or longer reaction time than 24 h and lower or higher temperature than 120 °C decelerated the reaction rate and led to lower yields (Table 2, entries 1-11). Use of CuO and γ -FeOOH individually generated the desired product in 16-18%

yield (Table 2, entries 1 and 2). The reaction is very slow in water; use of DMAc-water (1:1) mixture results in 3% yield indicating that this coupling process is fairly sensitive to water (Table 2, entry 7). In the absence of base, reaction fails completely (Table 2, entry 5). Among the several solvents tested, DMF, CH₃CN and DMSO were less effective compared to DMAc (Table 2, entries 1-4). Bases such as CS₂CO₃, K₃PO₄, K₂CO₃, KOH and K^t-OBu are found to facilitate the coupling reaction. Among them K₂CO₃ is the better base which gave good yield when compared to other bases (Table 2, entries 6-10). The N-arylation of imidazole is also found to be highly sensitive to reaction temperature and time. At lower temperature (30-90 °C) or lower reaction time (6-12 h), the reaction proceeds slowly or moderately (Table 2, entries 1-11). These preliminary results revealed that Fe-CuO is a good catalyst for N-arylation of imidazole in the presence of K₂CO₃ in DMAc solvent at 120 °C, which afforded the corresponding N-arylated product in 83% yield after 24 h (Table 2, entry 12). Once the conditions were found, other aryl halides were subjected to the same reaction under identical conditions and the results are presented in Table 3. Bromo is the better leaving group compared to chloro and fluoro groups (the leaving group ability of halogens is in the order of I > Br > Cl > F). Hence, the aryl bromides react faster compared to the aryl chlorides and fluorides (Table 3, entries 3, 10 and 11). It is noteworthy to mention that C-N cross-coupling reactions with aryl chlorides are rarely gave good yields. Even then, the aryl chlorides are also coupled with imidazole to afford the corresponding N-arylated products in excellent yields (Table 3, entries 7-10) which was not so in some other catalytic systems [43-44]. The *para*-substituted aryl halides provided a better yield in comparison to the *ortho*-substituted (Table 3, entries 4 and 11) aryl halides. The low yield of *ortho*-substituted aryl halides may be due to the steric effect²⁵. Kim et al., used CNTs supported CuO NPs as a catalyst for the N-arylation with the similar substrates under similar reaction conditions. But in many cases the present catalytic system showed higher activity. For instance the reaction of 4-chlorobenzoic acid with imidazole gave excellent yield 99% of N-arylated product in the present catalytic system (Table 3, entry 10) whereas the same product was obtained only to 88%²⁶. Punniyamurthy and co-workers⁴⁵ exploited the high surface area and reactive morphology of the CuO nanoparticles for successful C-N cross-coupling reactions.

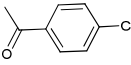
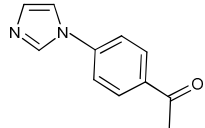
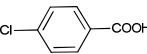
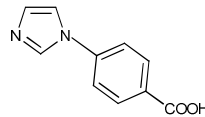
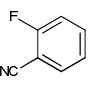
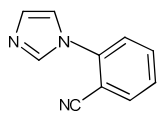
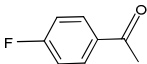
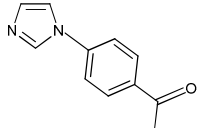
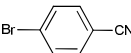
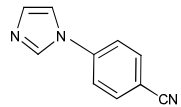
Although the results are promising, ligand free and easily separable for the N-arylation reaction but low yield were obtained in the N-arylated product coupling of aryl chlorides. Park and co-workers⁴⁶ used acetylene-carbon-immobilized CuO hollow nano spheres for N-arylation reactions at higher temperature (i.e.180°C) to get good yield and lower temperature than 180 °C led to lower yields but the present catalytic system excellent yields were obtained at 120°C. Usually C–F bond activation is not so easy; but the aryl fluorides are also coupled with imidazole to afford the corresponding N-arylated products in excellent yields (Table 3, entries 11 and 12). Especially, 4-fluoroacetophenone gave an excellent yield of 99% (Table 3,entry 12). Karvembu and co-workers reported that the CuO nanoparticles catalyzed C–N cross coupling of benzimidazole with 4-fluoroacetophenone to form N-arylated benzimidazole product under identical reaction conditions but the yield was low (67%)²⁵ as compared with the present catalytic system (99 %) (entry 11). Suramwar et al.,⁴⁷ reported the ligand-free copper oxide nanocatalyst for N-arylation of triazole with various aryl halides. They found that the Copper oxide catalyst showed very high conversions when the reaction was carried out in DMF or toluene as the solvent and difficulty in separation of product limits the method. No significant yield was observed with γ -FeOOH (Table 3, entry 13). Nevertheless the activity enhanced predominantly by the loading of CuO (Table 3, entries 1-12). Bimetallic systems generally showed better activity than monometallic systems⁴⁵⁻⁴⁸, which was evident in the present protocol as well. Niranjan et al., reported that the bimetallic system possesses a much higher surface area and hence much higher activity than those monometallic systems⁴⁹. A similar result was observed previously⁵⁰, in which Fe-Cu bimetallic system showed better catalytic performance than pure Fe₂O₃. Hence, many researchers involved in the development of bimetallic nanocomposite system for a targeted reaction⁵¹⁻⁵⁴. Notably, the Fe-CuO catalyst yielded the N-arylated imidazole product smoothly, which is promising and predominant over the previous reports⁵⁰. To expand the scope of this protocol further, other nitrogen containing heterocycles such as benzimidazole, carbazole, pyrrole, indole, and triazole are coupled with 4-bromobenzonitrile to give the corresponding N-arylated products in good yield (Table 4). In order to show that Fe-CuO nanoparticles are heterogeneous catalysts, a hot filtration

test was performed for N-arylation of imidazole with 4-bromo benzonitrile. In a typical experiment, the catalyst was separated out from the reaction mixture after 12 h by using a magnet, and then stirring was continued without the catalyst. The reaction was allowed to proceed further for 12 h and the yield was determined by GC at each 4 h intervals. The result indicated that no further conversion occurred after the nanocatalyst was separated out from the reaction mixture, which indicates that the N-arylation reaction of imidazole occurred only due to solid Fe-CuO (see ESI –S6†). Isolation and reuse of the catalyst are crucial requirements for any practical application in terms of cost and environmental protection. It is well known that magnetic separation makes the recovery of catalysts from the reaction medium much easier than the traditional separation procedures such as filtration and centrifugation. In the present system, the catalyst can be easily recovered by using an external magnet as shown in Fig. 1. Once the reaction was completed, the catalyst was trapped with the help of a magnet, washed with ethyl acetate, air dried and used directly in the next cycle. The catalyst could be reused six times without any significant detrimental effect on the yield (see ESI–S7†).

Surface area and particle size play a vital role in heterogeneous catalysis. Owing to the high active surface area of MNPs, they are usually employed as a heterogeneous nanocatalyst in various reactions and facilitate better yields. Particularly, MNPs having the size of fewer than 10 nm exhibited a dramatic catalytic activity⁵⁵. Therefore, the effect of Fe-CuO particle size on catalytic efficiency in terms of yields has been investigated. For this purpose, another nanocatalyst with Fe-CuO size of around 33 nm was prepared using the same procedure, but the calcinations were carried out at 500 °C for 3 h. It is well known that MNPs can easily agglomerate to form bigger particles particularly at higher temperature due to their high specific surface energy⁵⁶. Here, we postulate that the Fe-CuO might be agglomerated to form bigger Fe-CuO (33nm) at the calcination temperature of 500°C. The increase in the temperature from 30 to 500 °C increased the size of Fe-CuO from 7 nm to 33 nm; this suggests that the size of Fe-CuO depends on the calcination temperature. The Fe-CuO catalyst (33 nm) has a BET surface area of 50.31 m² g⁻¹ with a pore volume of 0.224 cm³ g⁻¹.

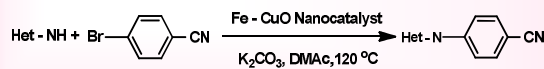
Table 3 Fe-CuO-catalyzed N-arylation of imidazole with various aryl halides^a

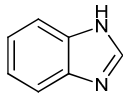
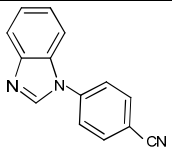
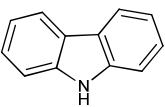
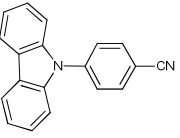
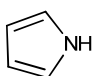
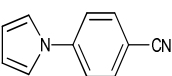
Entry	Aryl halides (1b)	Product (1c)	GC Yield (%)
1.			90 (68) ^b
2.			83 (77) ^b
3.			92 (84) ^b
4.			62 (59) ^b
5.			83 (82) ^b
6.			89 (83) ^b
7.			94 (90) ^b
8.			82 (78) ^b

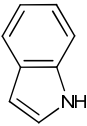
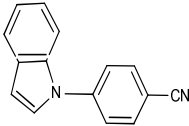
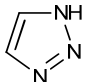
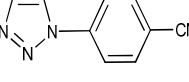
	9.			76 (57) ^b	
	10.			99 (89) ^b	
5	11.			74 (70) ^b	
10	12.			99 (94) ^b	
All	13. ^c			5 (3) ^b	the

reactions were performed with Fe-CuO (10 mg), 1 mmol (182 mg) of 4-bromobenzonitrile, 1.2 mmol (81 mg) of imidazole and 2.0 mmol of K₂CO₃ in 4 mL of solvent at 120 °C for 24 h. ^b Isolated yield. ^c Reaction performed with bare γ-FeOOH.

Table 4 Fe-CuO-catalyzed N-arylation of various heterocycles with 4-bromobenzonitrile^a

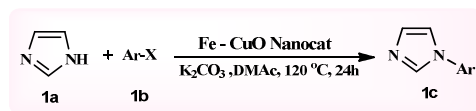


Entry	Het-NH	Product	Time (h)	Yield (%) ^b
1			20	72
2			24	83
3			24	98

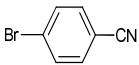
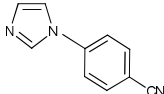
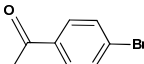
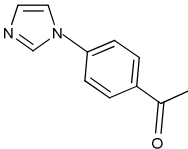
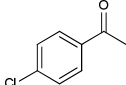
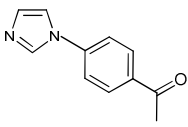
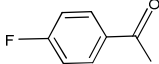
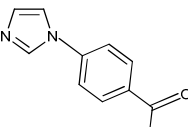
4.			16	65
5.			24	67

^a All the reactions were performed with Fe-CuO (10 mg), 1 mmol (182 mg) of 4-bromobenzonitrile, 1.2 mmol (81 mg) of heterocycles and 2.0 mmol of K₂CO₃ in 4 mL of solvent at 120 °C. ^bGCyield.

5 **Table 5** Catalytic activity of Fe-CuO (33 nm) and Fe-CuO (7 nm) toward N-arylation of imidazole with various aryl halides.



10

Entry	Ar-X (1b)	Product (1c)	Yield (%) ^b	Yield (%) ^c
1.			90	43
2.			92	56
3.			94	28
4.			99	47

^a All the reactions were performed with Fe-CuO (10 mg), 1 mmol (182 mg) of 4-bromobenzonitrile, 1.2 mmol (81 mg) of imidazole and 2.0 mmol of K₂CO₃ in 4 mL of DMAc at 120 °C for 24 h. ^b GC yield of the product when the particle size of Fe-CuO is 7 nm. ^c GC yield of the product when the particle size of Fe-CuO is 33 nm.

15

The surface area per unit mass (S) of 7 nm sized Fe-CuO was found to be 83.1989 m² g⁻¹ with a pore volume of 0.419 cm³ g⁻¹. Both the nanocatalysts were employed in the N-arylation reaction of imidazole with various aryl halides (Table 4). As expected, 7 nm Fe-CuO exhibited a good catalytic activity in comparison to the one which has 33 nm size (Table 5). When the size of Fe-CuO decreases, the surface area per unit mass (S) certainly increases. Consequently, a larger number of active sites are available. Thus, Fe-CuO having the particle size of 7 nm showed excellent catalytic activity.

A plausible three-step mechanism for the Fe-CuO-catalyzed N-arylation is proposed. The catalytic reaction is expected to take place *via* adsorption followed by desorption. In the first step, the aryl halide adsorbed over the surface of Fe-CuO nanocomposites to form intermediate-II. At the same time base removed proton from the imidazole which further displaced the halide ion from the surface of the catalyst. The imidazole anion attacks the phenyl cation to form N-arylated imidazole. In the final step the desired N-arylated imidazole product desorbed from the surface of the catalyst to complete the catalytic cycle.

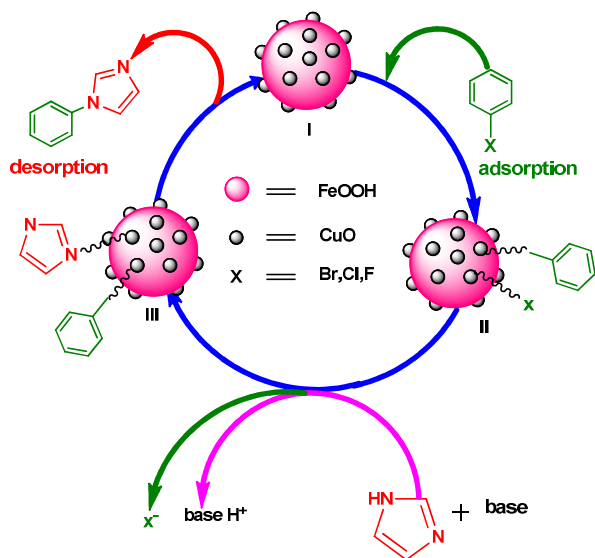


Fig. 13 Proposed mechanism for Fe-CuO-catalyzed N-arylation of imidazole with aryl halides

Conclusions

In summary a simple, highly efficient, economical, environmental friendly, easily separable and reusable heterogeneous Fe-CuO magnetic catalyst was prepared by a very simple precipitation technique. It showed good catalytic activity toward the N-

arylation of imidazole with various aryl halides. More significantly, this catalyst could be easily recovered by magnetic separation and reused for several cycles without significant loss of activity. This catalyst solves the basic problems of catalyst separation and recovery and thus this protocol may find widespread use for the preparation of N-arylated heterocycles.

Experimental Section

The reagents used in the synthesis, such as FeSO₄·7H₂O and CuSO₄ were purchased from Sigma-Aldrich and used as received without any further purification. ¹H NMR spectra were recorded at 250 and 400 MHz, and ¹³C NMR spectra were recorded at 62.9 and 100 MHz in CDCl₃ using TMS as an internal standard. Column chromatography was carried out on silica gel 60 Merck (230–240 mesh) in glass columns (2 or 3 cm diameter) using 15–30 grams of silica gel per one gram of the crude mixture. The morphology of the catalyst was investigated on scanning electron microscope (Hitachi COM-S-4200 SEM) and transmission electron microscope (Jeol, JEM-2100F TEM) with accelerating voltage of 120 kV. XRD analyses were performed on a Bruker D-8 Advance diffractometer using Cu K α radiation ($\lambda = 1.5418 \text{ \AA}$). The Fourier transform infrared (FT-IR) spectra were recorded (Jasco 460 Plus FT-IR) as KBr pellets in the wavenumber range 4000 - 400cm⁻¹. The oxidation state of the metals was determined by X-ray photoelectron spectroscopy (Kratos Axis-Ultra DLD, Kratos Analytical Ltd, Japan). The magnetic measurements were carried out on a vibrating sample magnetometer (Lakeshore, Model-7400) with an applied field between -15000 and 15000 (Oe) at room temperature. The Cu loading was determined by inductively coupled plasma optical emission spectrometry (ICP-OES, Élan DRC-e, and Perkin Elmer). Thermo gravimetric analysis was made with (SII EXSTAR 6200) TG/DTA analyzer. Raman spectrometer (Hololab 5000, Kaiser Optical Systems Inc.) was applied to examine the interaction between copper oxide nanoparticles (CuONPs) and lepidocrocite. The argon laser was operated at 532 nm with a Kaiser holographic edge. The specific surface area of the magnetic catalyst was determined by BET analysis while pore volume was determined by the Barrett–Joyner–Halenda (BJH) method using Quanta Chrome (NOVAe) surface area analyzer.

Preparation of Lepidocrocite

The lepidocrocite and Fe-CuO were prepared following a literature method²⁸. To prepare lepidocrocite, FeSO₄·7H₂O (0.13 M) was dissolved in distilled water (100 mL). Then NH₄OH

(10%) was added drop wise into the suspension until the pH of the solution was adjusted to 6.5. The mixture was stirred vigorously for 4 h. The black precipitate was collected from the solution by an external magnet and washed with double distilled water. Finally the black product was dried under vacuum at 80 °C.

Preparation of Fe – CuO catalyst

CuSO₄·5H₂O (0.005 M), was dissolved in distilled water (50 mL). γ-FeOOH (0.51 g) was then dispersed in the above solution and sonicated to obtain a uniform suspension. The suspension was vigorously stirred at room temperature for 50 min to ensure that enough Cu²⁺ had been adsorbed on the surface of γ-FeOOH. Then the pH was adjusted to 6.5 by adding 10% NH₄OH. The mixture was stirred vigorously for 4 h. The precipitated black product was collected from the solution using an external magnet (Figure 1), washed with water, and dried under vacuum at 80 °C.

Procedure for N-arylation of imidazole

In a typical procedure, Fe-CuO catalyst (10 mg) was added into a mixture of imidazole (1.2 mmol, 81 mg), 4-bromobenzonitrile (1 mmol, 182 mg) and K₂CO₃ (2 mmol, 276 mg) in DMAc (4 mL), stirred under air atmosphere at 120°C for 24h. After the complete consumption of starting materials as monitored by thin layer chromatography (TLC), the catalyst was separated by magnetic decantation and washed well with diethyl ether and dried in an oven at 110°C for 3h. The organic layer was partitioned between 10mL of ethyl acetate and 5mL of saturated aqueous NaCl solution. The product was extracted with ethyl acetate and dried over anhydrous sodium sulfate. The yield of product was determined by GC. Finally, the organic layer was concentrated to obtain N-arylated imidazole.

Product analysis

In order to confirm the formation of the product, samples of both reactants and products were dissolved in ethyl acetate and analyzed by gas chromatograph (Shimadzu 2010) equipped with 5% diphenyl and 95% dimethyl polysiloxane, Restek-5 capillary column (0.32 mm dia, 60 m length and 0.32 mm dia) and a flame ionization detector (FID). The initial column temperature was increased from 60 to 150 °C at the rate of 10 °C/min and then to 220 °C at the rate of 40 °C/min. N₂ was used as a carrier gas. During the product analysis the temperatures of the FID and injection port were kept constant at 150 and 250 °C respectively.

Acknowledgement

One of the authors R.S. is thankful to the Department of Science and Technology, Government of India, New Delhi for the award of research fellowship under the **DST PURSE** programme.

Notes and references

1. F. Diederich, A. de Meijere (Eds.), *Wiley-VCH, Weinheim.*, 2004.
2. J. P. Wolfe, S. Wagaw, J. F. Marcoux, S. L. Buchwald, *Acc. Chem Res*, 1998, **31**, 805.
3. G. R. Martinez, K. A. M. Walker, D. R. Hirschfield, J. J. Bruno, D. S. Yang, P. J. J. Maloney, *Med. Chem.*, 1992, **35**, 620.
4. J. Ohmori, M. S. Sasamata, M. Okada, S. Sakamoto, *J. Med. Chem.*, 1996, **39**, 3971.
5. I. Sircar, R. E. Weishaar, D. Kobylarz. H. Moos, J. A. Bristol, *J. Med. Chem.*, 1987, **30**, 1955.
6. P. Cozzi, G. Carganico, D. Fusar, M. Grossoni, M. Menichincheri, V. Pincioli, R. Tonani, F. Vaghi, P. Salvati, *J. Med. Chem.*, 1993, **36**, 2964
7. Y. S. Lo, J. C. Nolan, T. H. Maren, W. J. Jr. Welstead, D. F. Gripshover, D. A. J. Shamblee, *Med. Chem.*, 1992, **35**, 4790.
8. D. Maiti, B. P. Fors, J. L. Henderson, Y. Nakamura, S. L. Buchwald, *Chem. Sci.*, 2011, **2**, 57.
9. W. Yi, W. Zhiqing, W. Lixia, L. Zhengkai, Z. Xiangge, *Chem Euro J.*, 2009, **15**, 8971.
10. S. G. Babu, R. Karvembu. *Ind. Eng. Chem. Res.*, 2011, **50**, 9594.
11. M. L. Kantam, Y. Jagjit, L. Soumi, S. Bojja, J. Shailendra, *Adv. Synth. Catal.*, 2007, **349**, 1938.
12. S. Mandal, D. Roy, R. V. Chaudhari, M. Sastry, *Chem. Mater.*, 2004, **16**, 3714.
13. P. Poisson, J. P. Brunelle, P. Nortier, Catalyst Supports and Supported Catalysts, (Ed.: A. B. Stiles), Butterworth, Boston, 1987, pp. 11-55.
14. S. Shylesh, V. Schunemann, W. R. Thiel, *Angew. Chem., Int. Ed.*, 2010, **49**, 3428.
15. J. Fan, Y. Gao, *J. Exp. Nanosci.*, 2006, **1**, 457.
16. Y. Zhu, J. Shen, K. Zhou, C. Chen, X. Yang, C. Li, *J. Phys. Chem. C.*, 2011, **115**, 1614.
17. S. R. Kale, S. S. Kahandal, M. B. Gawande, R. V. Jayaram, *Rsc. Adv.*, 2013, **3**, 8184.
18. M. B. Gawande, P. S. Branco, R. S. Varma, *Chem. Soc. Rev.*, 2013, **42**, 3371.

19. R. B. N. Baig, R. S. Varma, *Chem. Commun.*, 2012, **48**, 2582.
20. P. H. Li, B. L. Li, Z. M. An, L. P. Mo, Z. S. Cui, Z. H. Zhang, *Adv. Synth. Catal.*, 2013, **355**, 2952.
- 5 21. M. J. Aliaga, D. J. Ramon, M. Yus, *Org. Biomol. Chem.*, 2010, **8**, 43.
22. M. Liu, X. G. Peng, W. Sun, Y. W. Zhao, C. G. Xia, *Org. Lett.*, 2008, **10**, 3933.
23. S. G. Babu, P. A. Priyadarsini, R. Karvembu, *Appl. Catal. A: Gen.*, 2011, **392**, 218.
- 10 24. S. G. Babu, R. Karvembu, *Tetrahedron Lett.*, 2013, **54**, 1677.
25. S. G. Babu, R. Karvembu, *Ind. Eng. Chem. Res.*, 2011, **50**, 9594.
- 15 26. M. Gopiraman, S. G. Babu, Z. Khatri, W. Kai, Y. A. Kim, M. Endo, R. Karvembu, I. S. Kim, *Carbon.*, 2013, **62**, 135.
27. D. Takagi, Y. Homma, H. Hibino, S. Suzuki, Y. Kobayashi, *Nano Lett.*, 2006, **6**, 2642.
28. K. Inouye, K. Ichimura, K. Kaneko, T. Ishikawa, *Corro. Sci.*, 1976, **16**, 507.
- 20 29. R. M. Cornell, U. Schwertmann, *The Iron Oxides*, second ed., *VCH, New York.*, 2003
30. M. Ristic, S. Music, M. Godec, *J. Alloys Compd.*, 2006, **417**, 292.
- 25 31. G. Socrates, *John Wiley & Sons Ltd, New York.*, 2001.
32. D. Liu, S. Yang, S. T. Lee, *J. Phys. Chem. C.*, 2008, **112**, 7110.
33. S. Rahman, K. Nadeem, M. A. Rehman, M. Mumtaz, S. Naeem, I. L. Papst, *Ceram. Int.*, 2013, **39**, 5235.
- 30 34. T. Yamashita, P. Hayes, *Appl. Surf. Sci.*, 2008, **254**, 2441.
35. J. Ghijsen, L. H. Tjeng, J. Van, H. Eskes, J. Westerink, G. A. Sawatzky, M. T. Czyzyk, *Phys. Rev. B.*, 1988, **38**, 11322.
- 75 36. N. S. McIntyre, M. G. Cook, *Anal. Chem.*, 1975, **47**, 2208.
37. M. Hanesch, *Geophys. J. Int.*, 2009, **177**, 941.
- 35 38. J. F. Xu, W. Ji, Z. X. Shen, W. S. Li, S. H. Tang, X. R. Ye, D. Z. Jia, X. Q. Xin, *J. Raman Spectrosc.*, 1999, **30**, 413.
39. A. V. Shchukarev, D. V. Korolkov, *Cent. Eur. J. Chem.*, 2004, **2**, 347.
- 80 40. D. L. A. de Faria, S. V. Silva, M. T. de Oliveira, *J. Raman Spectrosc.*, 1997, **28**, 873.
- 40 41. Y. Zhu, K. Mimura, M. Isshiki, *Mater. Trans.*, 2002, **4**, 2173.
- 85 42. K. Inouye, K. Ichimura, K. Kaneko, T. Ishikawa, *Corros. Sci.*, 1976, **16**, 507.
- 45 43. H. J. Cristau, P. P. Cellier, J. F. Spindler, M. Taillefer, *Eur. J. Org. Chem.* 2004, **256**, 695.
44. M. Taillefer, N. Xia, A. Ouali, *Angew. Chem., Int. Ed.* 2007, **46**, 934.
45. L. Rout, S. Jammi, T. Punniyamurthy, *Org. Lett.* 2009, **74**, 3397.
- 50 46. A. Y. Kim, H. J. Lee, J. C. Park, H. Kang, H. Yang, H. Song, K. H. Park, *Molecule*, 2009, **14**, 5169.
47. N. V. Suramwar, S. R. Thakare, N. T. Khaty, *J. Mol. Cat. A*, 2012, **359**, 28.
- 55 48. J. A. Rodriguez, *Surf. Sci. Rep.*, 1996, **24**, 223.
49. P. Niranjana, J. A. Kumar, M. Sasmita, R. S. M. Ranjan, *Tetrahedron Lett.*, 2011, **52**, 1924.
50. W. M. Shaheen, *Mater. Sci. Eng. A*, 2007, **445**, 113.
51. I. E. Wachs, *Catal. Today.*, 2005, **100**, 79.
- 60 52. M. Taillefer, N. Xia, A. Ouali, *Angew. Chem., Int. Ed.* 2007, **46**, 934.
53. Z. Wang, H. Fu, Y. Jiang, Y. Zhao, *Synlett* 2008, 2540.
54. D. Guo, H. Huang, Y. Zhou, J. Xu, H. Jiang, K. Chen, H. Liu, *Green Chem.* 2010, **12**, 276.
- 65 55. G. A. E. Shobaky, N. M. Deraz, *Mater. Lett.*, 2001, **47**, 231
56. S. H. Joo, J. Y. Park, J. R. Renzas, D. R. Butcher, W. Huang, G. Somorjai, *Nano Lett.*, 2010, **10**, 2709.
57. A. T. Bell, *Science*, 2003, **299**, 1688.